ASEAN Journal of Chemical Engineering 2024, Vol. 24, No. 2, 186 – 199

Synthesis of Green Diesel from Non-edible Kapok *(Ceiba pentandra)* Seed Oil via Hydrotreating Process Using Sulfided Ni-Mo/γ-Al_2O_3 Catalysts

Tedi Hudaya[*,1]
Sarah Amadea Rahardja[1]
Michael Gunawan[1]
Tatang Hernas Soerawidjaja[2]
[1]*Chemical Engineering Department, Parahyangan Catholic University, Jalan Ciumbuleuit 94 Bandung, Indonesia.*
[2]*Chemical Engineering Department, Bandung Institute of Technology, Jalan Ganesha 10 Bandung, Indonesia*
*e-mail: t.hudaya@unpar.ac.id

Submitted 26 February 2024 *Revised* 12 July 2024 *Accepted* 28 July 2024

Abstract. The demand for environmentally friendly and renewable fuels will keep increasing due to the accelerated climate change worldwide. *Ceiba pentandra* seed oil is a promising feedstock for renewable fuel since it possesses major fatty acid components with similar skeletal structure to diesel-range hydrocarbons. Nevertheless, its direct utilization will potentially cause problems due to the cyclopropenoid group and its high viscosity. In this research, hydrotreating processes over bimetallic sulfided Ni-Mo/γ-Al_2O_3 catalysts were performed to convert the kapok seed oil into green diesel, with lower cloud points compared to those derived from other common vegetable oils. The hydrotreating process was needed not only to eliminate cyclopropenoid and oxygen contents but also to reduce the unsaturated bonds and, at the same time, increase its H/C ratio. The BET measurement showed the catalyst surface area of 144 m^2/g, while the existence of NiS and MoS_2 as active sites on its surface was detected by XRD analysis. The TEM analysis indicated that sulfided Ni and Mo were dispersed reasonably well, with a little aggregation, on the catalyst surface. The most well-performed catalyst (with Ni:Mo ratio of 0.2:1 and K:P promoter ratio 0.5:1) successfully synthesized bio-hydrocarbons (with desirable C_{15}-C_{19} diesel range) with the conversion of almost 96%, with no remaining cyclopropenoid content.

Keywords: Green Diesel, Hydrotreating, Kapok Seed, Non-edible Oil, Sulfided NiMo/γ-Al_2O_3

INTRODUCTION

The massive and continuous exploitation of petroleum as primary fossil fuels has seriously impacted the environment and human beings. The steady increase of CO_2 up to the current dangerous level (around 420 ppm) in the atmosphere, mainly due to the combustion of fossil-based fuels, is truly problematic and unsustainable from many perspectives. Therefore, the development of renewable and more sustainable fuel has received more and more attention in recent years. Fatty Acid Methyl Ester (FAME) or well-

DOI: 10.22146/ajche.12348

known as biodiesel has been an attractive alternative solution to ease today's environmental problem caused by excessive petroleum usage.

Nevertheless, the production of FAME usually requires vegetable oils as feedstock, such as soybean and palm oil (Issariyakul & Dalai, 2014). Using such edible oils raised the concern of a possible competition between food with oleochemicals and energy sectors, which receded biodiesel development. To overcome this challenge, some researchers try to look for alternative non-edible feedstocks for biofuel production, such as kapok (*Ceiba pentandra*) seed oil, because it contains approximately 24.3%-wt palmitic acid, 21.9%-wt oleic acid, and 38.9%-wt linoleic acid as major components (Table 1), which perfectly falls in the range of diesel hydrocarbons. Kapok is a tree that grows easily and is widely cultivated in Indonesia for its fiber. However, the oil is not commonly well utilized. Besides its compositions, which are in the diesel range, the utilization of *Ceiba pentandra* seed oil (as a non-edible oil) will not cause any food versus energy competition in the future.

The direct usage of kapok seed oil as fuel is not feasible because of its high viscosity as well as the cyclopropenoid (typically about 10%) content as malvalic and sterculic acids. The cyclopropenoid group itself is highly reactive, thus its presence can lead to dimerization and oligomerization of carbon chains (Harris, 1982; Tedi Hudaya, 2013) . This phenomenon can cause the blocking of the injection nozzle in a diesel machine. Therefore, the hydrotreating process of the kapok seed oil is needed not only to eliminate cyclopropenoid and oxygen contents but also to reduce the unsaturated bonds and, at the same time, increase its H/C ratio to convert the raw kapok seed oil into green diesel. Two advantages are obtained in comparison to the FAME route: firstly, the resulting green diesel is a 'drop-in' fuel that may substitute up to 100% petroleum diesel. Secondly, the green diesel will have a lower cloud point (due to methyl branch presence as illustrated in Figure 1) than those derived from other common vegetable oils such as palm, canola, or corn oils.

Table 1. Typical fatty acid compositions in kapok seed oil (Berry, 1979)

Fatty Acid	Content (%) *
Palmitic acid ($C_{16:0}$)	22.37 ± 0.50
Stearic acid ($C_{18:0}$)	3.80 ± 0.12
Oleic acid ($C_{18:1}$)	23.24 ± 0.41
Linoleic acid ($C_{18:2}$)	33.63 ± 0.50
Malvalic acid	9.14 ± 0.10
Sterculic acid	2.58 ± 0.15
Behenic acid ($C_{22:0}$)	0.46 ± 0.05

* Values are means ± SD of three different seed oil samples. Each analyzed independently in triplicate (n = 3x3)

The Hydrotreating process involves a three-phase reaction system in which the liquid (oil) feed is mixed with a solid catalyst in the presence of H_2 gas. The hydrotreating reaction consist of the hydrogenation of unsaturated C=C bonds in kapok seed oil (Eq. 1) as the first step, including the elimination of cyclopropenoid groups in kapok seed oil (Figure 1) through the addition and ring opening reactions of the cyclopropenoid group which resulting in a favorable branched-chain fatty acid structure which may later contribute to the lower cloud point of the hydrocarbons products (Hudaya *et al.*, 2013).

The second step is involves the breaking of (hydrogenolysis) ester group resulting in fatty acids and propane and then followed by oxygen removal (deoxygenation) within fatty acid molecules via three possible reactions, which are hydrodeoxygenation (Eq. 2), decarboxylation (Eq. 3) and decarbonylation (Eq. 4) (Wang, 2012). The reactions' stoichiometry is as follows:

$R_1C=CR_2 + H_2 \rightarrow R_1HC–CHR_2$ (1)

$RCOOH + 3\ H_2 \rightarrow RCH_3 + 2\ H_2O$ (2)

$RCOOH \rightarrow RH + CO_2$ (3)

$RCOOH + H2 \rightarrow RH + CO + H_2O$ (4)

Theoretically, the hydrodeoxygenation process (Eq. 2) consumes more hydrogen than the rest of the deoxygenation reactions (Eq. 3 and 4). Hydrodeoxygenation needs 3 moles of hydrogen for each mol of bio-hydrocarbon produced, meanwhile the decarbonylation needs only 1 mol of hydrogen and the decarboxylation even does not consume hydrogen at all. From another point of view, however, the decarbonylation and decarboxylation routes are slightly unfavorable because the bio-hydrocarbon produced will lose one Carbon atom, which is released as CO and CO_2 (Antoine Daudin, 2013; Ramin Abhari, 2011), marginally reducing its caloric value.

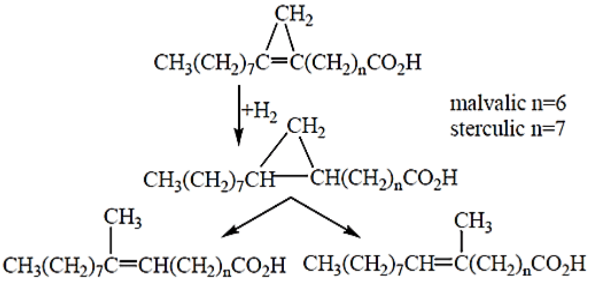

Fig. 1: The hydrogenation of cyclopropenoid group which started by the double-bond saturation (step 1) and followed by ring opening reaction (step 2), resulting in branched-chain fatty acid structures.

Sulfided Ni-Mo catalyst was widely developed and used as an effective catalyst for the hydrotreating of vegetable oil (David Kubicka, 2010; Hasan Dindi, 2008; Makoto Toba, 2011; Masita Mohammad, 2013; T.V. Choudhary, 2011; Wang, 2012). The nickel active site was reported for its high selectivity towards the decarboxylation process as well as its high activity in the hydrogenation process (Hasan Dindi, 2008; Ramin Abhari, 2011). Meanwhile molybdenum content was reported for its selectivity toward hydrodeoxygenation process (Vonortas A., 2014). In addition, the sulfided form of the metal active sites was required to maintain the catalyst activity in deoxygenation on sulfided hydrotreating catalysts (Senol *et al.*, 2007). Therefore, an optimum combination of Ni-Mo as a hydrotreating catalyst would result in not only a high yield of bio-hydrocarbon production but also a reasonable hydrogen consumption.

Potassium (K) and phosphorous (P) promoters were often used to improve the performance of the sulfided Ni-Mo catalyst. Promoters are substances that are not catalytically active but may increase the activity of catalysts (Hagen, 2006). Potassium promoter was used to prevent coke formation on active centers because it could partly neutralize the acid center of the catalyst (Hagen, 2006; Martina Chiappero, 2011) which could promote undesirable cracking reactions with coke as the by-product. Meanwhile, the phosphorus promoter was used to increase the stability of the catalyst, weaken metal-support interaction, and increase the molybdenum dispersion on the catalyst surface, but unfortunately, it might increase the acidity of the catalytic system (Paolina Atanasova, 1988; Ryuichiro Iwamoto, 1999). Therefore, an appropriate amount and ratio of the promoters added to the catalyst formula is one of the keys to getting a desirable performance of the catalytic system.

This research aims are to convert kapok seed oil into a low cloud point green diesel, i.e., bio-hydrocarbon in diesel fuel range, via hydrotreating processes. Specifically, the effect of the Ni:Mo and K:P ratios (in various sulfided Ni-Mo/γ-Al_2O_3 catalysts) on the catalyst activity towards hydrotreating processes and green diesel properties were also investigated in this research. The catalyst formulae which resulted in the best performance was then characterized for BET area, XRD, and TEM analyses.

MATERIALS AND METHODS

The synthesis of green diesel from kapok seed oil involved three main steps: catalyst preparation, kapok seed oil pre-treatment, and the hydrotreating process of the oil.

Catalyst Synthesis

The precursor solution was prepared by dissolving ammonium heptamolybdate tetrahydrate and nickel (II) nitrate hexahydrate with varied mole ratios of Ni:Mo (0.2:1, 0.33:1, and 0.4:1) in RO water. The Ni content was ranging 1.62-2.59 %-w, while the Mo content was 10.55-13.16%-w. Phosphorus acid as the source of the P promoter was also added to the precursor solution concurrently with either KOH or K_2CO_3 as the source of the K promoter. The weight ratio of KOH (or K_2CO_3) as K promoter to H_3PO_4 as P promoter also varied (0.25:1 and 0.5:1). The K promoters' content was only a few percent of the total weight of the catalyst. The complete list of catalyst variations and their denotations is shown in Table 2. The total mass of the catalyst precursors was between 7.4475 – 7.5350 grams (RO water as the solvent was excluded).

The solution was then incorporated into the support using the incipient wetness impregnation method for 1 hour. This method was widely used to effectively prepare the impregnation of both active sites and promoters onto the alumina support. Before the precursor solution was impregnated onto catalyst support, the γ-Al_2O_3 granule was dried at 120 °C for 2 hours. The precursor solution was added onto the catalyst until all the catalyst support pore volume was filled. After the impregnation step, the catalyst was dried at 120 °C for 15 hours, and then calcined in an air stream at 550 °C for 5 hours.

Furthermore, the active and sulfided forms of the catalyst were obtained by sulfiding the catalyst at 425 °C. The sulfidation was conducted in a quartz tubular reactor, where the catalyst was put on the catalyst support made from glass wool. Firstly, an excess amount of CS_2 solution was placed onto a small crucible above which a hydrogen stream of 75 ml/min at 2 bars was passed through before entering the reactor. The hydrogen reacted with CS_2, resulting in H_2S and CH_4. The catalyst was then sulfided using H_2S gas flowing through a catalyst bed maintained at 425 °C. The excess H_2S gas was captured and then neutralized in a scrubber vessel, which contained 10% NaOH solution.

Table 2. Catalyst variation denotation

Catalyst	***Variation***		
	K Promoter	*Ni : Mo mole ratio*	*KOH/K_2CO_3 to H_3PO_4 weight ratio*
1	*K_2CO_3*	*0.2*	*0.25*
2	*KOH*	*0.2*	*0.25*
3	*K_2CO_3*	*0.33*	*0.25*
4	*KOH*	*0.33*	*0.25*
5	*K_2CO_3*	*0.4*	*0.25*
6	*KOH*	*0.4*	*0.25*
7	*K_2CO_3*	*0.2*	*0.5*
8	*KOH*	*0.2*	*0.5*
9	*K_2CO_3*	*0.33*	*0.5*
10	*KOH*	*0.33*	*0.5*
11	*K_2CO_3*	*0.4*	*0.5*
12	*KOH*	*0.4*	*0.5*

Raw Oil Pre-Treatment

Pre-treatment steps consist of degumming and bleaching processes to reduce the kapok seed oil's oxidation tendency and eliminate impurities such as phospholipids, iron or other metals that might be present in the form of metal-phosphatide complexes, and also some color pigments (Varpu Markkanen, 2010).

Kapok seed oil was heated to 80-90 °C on a hotplate and stirred using a magnetic stirrer. After the desired temperature was reached, phosphorus acid (85%) was subsequently added into the oil as much as 0.25% (v/w) under stirring for 20 minutes. 5% (v/v) distilled water was added and the mixture was then introduced into a separating funnel, which was allowed to settle for 30 minutes. The bottom layer was drained through the bottom valve, and the oil in the upper layer was subsequently washed several times to remove the impurities and remaining acids completely. The remaining water in oil was subsequently detached by centrifugation at 5000 rpm for 30 minutes. The oil was later heated up to 90°C and then 3% of bleaching earth was added into the oil and mixed for 30 minutes. Then, the clean oil and bleaching earth were separated by centrifugation similarly.

Hydrotreating

Pre-treated kapok seed oil and 3% of catalyst (sulfided Ni-Mo/γ-Al_2O_3) were introduced into a high-pressure stainless-steel batch reactor with a 175 mL capacity (50 mm diameter and 90 mm height). The reactor was equipped with a glass-covered magnetic stirrer, an electrical heater, and a cooling fan. A PID temperature controller was used to maintain the reaction temperature without significant fluctuation or overshot.

Initially, nitrogen gas purging was conducted to remove air in the reactor to prevent any explosion due to the reaction between hydrogen and oxygen. For safety reasons, a thorough leak test was also conducted each time to ensure no leakage from the reactor to the environment.

As previously described, hydrotreating was carried out in two steps, namely hydrogenation and deoxygenation. Hydrogen gas was initially introduced to the reactor until 1.7 MPa, and the reactor was subsequently heated up to 250 °C (with final pressure of 3 MPa), and the reaction was allowed for 2 hours for the hydrogenation process. After the hydrogenation reaction finished, some additional hydrogen was added, and then the temperature of the reactor was increased to 340 °C (with final pressure of 5 MPa) for the deoxygenation reaction, which took place for 4 hours.

The product of the hydrotreating process was separated by centrifugation at 6000 rpm for 20 minutes to separate the catalyst from the bio-hydrocarbons. The catalyst was then washed using n-hexane several times to eliminate the remaining or trapped bio-hydrocarbons on its surface and then heated for several hours to remove the n-hexane. Some (selected) spent/used catalyst samples were then analyzed by using the Energy Dispersive X-ray Spectroscopy (EDS) machine Hitachi SEM SU3500 to determine the amount of coke deposited (as the cracking by-product) on its surface. The bio-hydrocarbons mixture was finally tested for its density and viscosity, as well as iodine and saponification values, and further analyzed by Gas Chromatography (Shimadzu) for its composition. The cyclopropenoid presence in the bio-hydrocarbons product was identified qualitatively by using the Besson test and Fourier Transform Infrared Spectroscopy (Shimadzu IR Affinity 1 S) and also quantitatively (titrimetrically) using the

Dubertaki reagent.

The catalyst formulae which resulted in the best performance i.e., high performance in the hydrogenation (indicated by a low iodine value) and deoxygenation (indicated by a low saponification value in the final product) as well as cyclopropenoid group removal, was further examined by X-ray diffraction (XRD - PANalytical Aeris) and transmission electron microscopy (TEM) analysis using Tecnai G2 20S-Twin. Meanwhile its surface area was measured using Brunauer-Emmett-Teller (BET) method using Quantachrome Nova 4200e.

RESULTS AND DISCUSSION

Characterization of Kapok Seed Oil

To provide a benchmark against processed oils, some tests were conducted to identify the characteristics and physical properties of raw kapok-oil. As one of the key parameters, the density of the oil was measured by using the pycnometer method. While the Besson test and titration by Dubertaki reagent were done to identify and quantify the cyclopropenoid content in the kapok raw oil. In addition to that, the iodine value of the oil was determined to measure the degree of unsaturation of the oil according to the Wijs method. The characteristic and physical properties of kapok-oil are shown in Table 3.

Catalyst Performance

The sulfided Ni-Mo/γ-Al_2O_3 catalyst synthesized and used in this research gave different performances depending on the treatment given to the catalyst. The result of this research is shown in Table 4. The effect of the Ni:Mo ratio, K promoter source, and the ratio between K and P promoter will be explained in points 3.2.1, 3.2.2, and 3.2.3, respectively.

Table 3. Characteristic and physical properties of kapok-oil

Properties	Unit	Specification
Colour	-	dark yellow
Density	kg/m^3	915.2
Cyclopropenoid content	mmol/g-oil	0.4647 (13.03% as malvalic acid or 13.68% as sterculic acid)
Iodine value	g-I_2 /100 g-oil	92.84
Saponification value	g-KOH/100 g-oil	204.4

The Effect of Ni:Mo Ratio

Based on the experimental results in Table 4, the effect of the Ni:Mo ratio on the catalyst performance could be analyzed. Generally, the increase of the Ni:Mo ratio would result in a slight decrease in the conversion of kapok oil, increasing the iodine value as well as cyclopropenoid remains in the hydrocarbon products. Ameen *et al.* (2020) reported that excess nickel content might lead to a lower extent of decarboxylation. Furthermore, excessive nickel can also lead to Ni particles agglomeration on the catalyst's surface (Wua *et al.*, 2020), which can result in fewer active sites available for the reactions. According to Ding *et al.* (2020), the active site's edge with a low Ni-Mo ratio on the catalyst surface favors the selective adsorption of olefin, which will then undergo a smooth conversion to alkanes via a series of elementary reactions.

In addition, the EDS results of spent catalysts indicated that a higher Ni:Mo ratio had more carbon elements than the catalyst with a lower ratio. For example, the spent catalyst 11 with a Ni:Mo ratio of 0.4 contained 27.2% of carbon, while spent catalyst 9 with a Ni:Mo ratio of 0.33 consisted of 22.5% of carbon. Hence, the catalyst deactivation due to carbon deposit on high Ni:Mo catalyst was

Table 4. Properties of bio-hydrocarbon formed

Experiment	**(1)**	**(2)**	**(3)**	**(4)**	**(5)**	**(6)****
Density	779.2	778.8	786.3	801.8	785.5	-
Kinematic viscosity	4.43	4.50	4.64	-	4.37	-
Iodine value	23.45	30.21	39.18	44.85	40.91	-
Saponification value	16.8	19.6	22.4	33.6	28	-
Conversion	91.78	90.41	89.04	83.56	86.30	-
Final cyclopropenoid	0	0.002 (99%removal)	0	0.02 (96%removal)	0	-
Besson test	(-)	(-)	(-)	(-)	(-)	-
Experiment	**(7)**	**(8)**	**(9)**	**(10)**	**(11)**	**(12)**
Density	780.5	776.6	780.5	781.8	778.2	796
Kinematic viscosity	4.37	4.01	4.04	4.27	4.18	-
Iodine value	21.56	13.38	19.67	21.24	29.11	39.18
Saponification value	14	8.4	8.4	14	19.6	30.8
Conversion	93.15	95.89	95.89	93.15	90.41	84.93
Final cyclopropenoid	0	0	0.002	0.001	0.002	0.02
Besson test	(-)	(-)	(-)	(-)	(-)	(-)

* The unit involved: density (kg m^{-3}), kinematic viscosity (mm^2 s^{-1}), Iodine value (g-I_2/100 g-oil), saponification value (g-KOH/100 g-oil), conversion (%), cyclopropenoid content (mmol/g-oil)

** The physical properties of the product with catalyst 6 could not be analyzed because the product turned to gel at room temperature, viscosity of products with catalyst 4 & 12 were not measured as the products were solid-liquid mixture

also responsible for the lower conversion to bio-hydrocarbons

Based on product distributions as shown in Table 5, the catalyst with Ni:Mo ratio of 0.4:1 (catalysts 5, 6 and 11, 12) tends to show a wider range of products (C_{14}-C_{30}). Meanwhile, the Ni:Mo ratio of 0.2:1 (catalysts 1, 2 and 7, 8) resulted in diesel-range hydrocarbons products (C_{14}-C_{19}, in which a majority portion or >80% consisted of C_{15}-C_{18} hydrocarbons). These results showed that catalysts with a higher Ni:Mo ratio tend to initiate dimerization reactions, which then create undesired heavy (up to C_{30}) hydrocarbon products. The highly reactive terminal alkene (detected by FTIR analyses) was the precursor for the dimerization reaction. Santillan-Jimenez & Crocker (2012) found that the nickel content in similar catalysts accelerated decarbonylation reaction rate, resulting in a terminal alkene-containing product. Therefore, an excessive amount of nickel in the catalyst could definitely have a negative impact on the catalyst's ability to convert vegetable oil through hydrogenation and deoxygenation reactions. The best Ni:Mo ratio catalyst under investigation was 0.2:1 (in which the Ni content was the lowest at 1.62% and the highest Mo content of 13.16%), which resulting higher conversion (90.41 – 95.89%), lower iodine value (13.38 – 30.21) and without any remaining cyclopropenoid content found in the products.

Hydrogen gas consumption at the early hydrogenation step could be associated with the saturation process of the double bonds, especially targeting the highly reactive cyclopropenoid group. In addition, the hydrogenolysis reaction between triglycerides and H_2 to produce fatty acids and propane typically occurs at temperatures between 200°C to 300°C, with a Ni catalyst. The pressure changes during the hydrogenation were recorded, and in most of the runs, the pressure drops were significant, about 10-15 bars within 2 hours of the reaction period. The pressure drops showed that the hydrogenation could successfully be carried out, supported by the significant (between 52-86%) reduction of Iodine numbers.

Table 5. GC analysis results

	Experiment	**(1)**	**(2)**	**(3)**	**(4)**	**(5)**	**(6)⁺**
Composition (%-mol)	C14 – C 15	1.32	2.36	3.54	4.35	3.84	-
	C15 – C 16	16.37	15.28	12.29	12.17	16.35	-
	C16 – C 17	59.74	18.20	16.66	23.98	13.95	-
	C17 – C 18	4.88	46.66	36.74	40.99	48.73	-
	C18 – C 19	17.69	17.50	7.60	12.73	-	-
	C19 – C 20	-	-	1.55	2.90	1.45	-
	C20 – C 21	-	-	1.39	2.88	1.38	-
	C21 – C 22	-	-	2.27	-	5.01	-
	C22 – C 23	-	-	1.47	-	-	-
	C23 – C 24	-	-	4.79	-	2.75	-
	C24 – C 25	-	-	4.41	-	-	-
	C25 – C 26	-	-	3.48	-	2.29	-
	C26 – C 27	-	-	2.28	-	2.27	-
	C27 – C 28	-	-	1.52	-	-	-
	C29 – C 30	-	-	-	-	1.98	-
	Experiment	**(7)**	**(8)**	**(9)**	**(10)**	**(11)**	**(12)**
Composition (%-mol)	C14 – C 15	1.81	-	1.22	1.76	-	19.48
	C15 – C 16	23.67	16.10	24.25	23.78	17.35	3.82
	C16 – C 17	8.50	13.58	8.33	9.06	12.76	16.22
	C17 – C 18	50.33	51.43	54.54	53.16	53.64	49.77
	C18 – C 19	15.69	18.89	11.66	12.25	16.26	-
	C19 – C 20	-	-	-	-	-	2.39
	C21 – C 22	-	-	-	-	-	4.02
	C22 – C 23	-	-	-	-	-	1.6
	C23 – C 24	-	-	-	-	-	1.44
	C24 – C 25	-	-	-	-	-	1.26

⁺ The product of run with catalyst 6 can’t be analyzed because the product turn to gel at room temperature

Another interesting result was that some runs produced green diesel products with white precipitates (for example, runs with catalysts 6 and 12), showed relatively lower pressure drops compared to the remaining runs. It was suspected that the imperfection of the hydrogenation process might lead to more extensive dimerization since chains containing reactive double bonds were easily able to react with each other. As previously discussed, an excessive amount of nickel in the catalyst could negatively impact the catalyst's ability to convert vegetable oil through hydrogenation and later deoxygenation reactions.

Furthermore, the pressure drop could be the selectivity indicator between hydrodeoxygenation and decarboxylation reactions. Referring to reactions (2) and (3), hydrodeoxygenation (2) would bring down the total gas pressure, because the moles of gas on the product side were less than the gas moles on the reactant side. On the contrary, for decarboxylation reaction (3), the opposite would happen or the increasing total gas pressure. All the runs gave a pressure drop of about 20 bars, which showed all the catalyst samples, in which Ni:Mo ratio ≥ 0.2, had higher selectivity towards hydrodeoxygenation rather than decarboxylation, which might be related to much higher Mo content (10.55-13.16%-w) than Ni content (1.62-2.59 %-w) in the catalyst formula. Furthermore, an increasing nickel content (from Ni:Mo ratio 0.2 to 0.4) on the catalyst would increase the decarboxylation reaction portion, indicated by a lower pressure drop, as it had been confirmed by (Hasan Dindi, 2008; Ramin Abhari, 2011).

Based on the above-discussed observations, a higher Ni:Mo ratio in the catalyst leads to lower conversion due to catalyst deactivation caused by carbon formation. Moreover, the nickel active sites accelerate the decarbonylation catalyst, which produces more terminal-alkene-containing hydrocarbons. Such reactive hydrocarbons tend to undergo dimerization and produce undesirable heavy hydrocarbons.

The Effect of K Promoter Source

The K promoter was purposely added to reduce the acidity of the alumina support, and thus hopefully minimize the tendency of coke formation on the catalyst. Coking results from the cracking reaction on Brønsted acid centers, followed by an acid-catalyzed polymerization to give $(CH_x)_n$ chains, which later cover the active centers on the catalyst surface and may also block the pores (Hagen, 2006).

An interesting finding was found from selected used catalyst samples using EDS analyses for catalysts 11 and 12, which had similar potassium loadings using K_2CO_3 and KOH as potassium promoter sources, respectively. The content of Carbon from the coke deposit on the catalyst 11 surface was 27.21%, lower than on catalyst 12 at 31.13% C. This amount of coke formed indicated that if compared to KOH, K_2CO_3 salt slightly better in preventing coke formation. Consequently, catalyst 11 gave a better performance (Table 4) in terms of Iodine value (removal of C=C) as well as oil conversions to hydrocarbons. However, the GC analysis (Table 5) indicates no considerable differences in the bio-hydrocarbons product's chain length distribution between catalysts with KOH and K_2CO_3 promoters.

The Effect of K:P Promoter Ratio

The amount of K and P promoters added must be optimized for the best catalyst performance. A finding was observed from this research that the higher K:P promoter ratio (0.5) resulting higher conversions of kapok-oil (84.9 – 95.9%) if compared to the lower one (0.25), which resulting lower conversions of kapok-oil (83.6 – 91.8%). The higher amount of K promoter (in the ratio of K:P of 0.5:1) also gave a smaller iodine value (13.38 – 39.18 g-I_2/100 g), in the saturation of kapok-oil, if compared to the smaller amount of K promoter (23.45 – 44.85 g-I_2/100 g).

In terms of hydrocarbons formed, the lower K:P promoter (0.25) generally gave a higher tendency of long-chain C_{22} – C_{30} hydrocarbons formation. Especially for higher Ni:Mo ratio (0.33 and 0.4) with promoter K_2CO_3, the hydrocarbons formed (catalyst no 3 and 5 in Table 5 above) contained C_{22+} hydrocarbon chains (fatty acids in original kapok seed oil had maximum C of 22). The C_{22+} hydrocarbon chains might have been formed by the dimerization of carbon chains with terminal double bonds (terminal alkene), which were very reactive, as shown by more viscous liquid and either precipitates or partial gel formation. For catalysts using KOH as the promoter, similar results were observed while a high ratio of Ni:Mo (0.33 and 0.4) was employed, especially for catalyst no 6; a detrimental result was obtained since the product was completely becoming a gel. This similar phenomenon was also observed, even at a high level (ratio 0.5) of K promoter at the highest Ni:Mo ratio of 0.4, i.e., for catalyst no 12. Therefore, a combination of high Ni:Mo and insufficient K promotor might lead to undesirable products in terms of hydrocarbon chain distribution, which was beyond the desired diesel-like range.

In addition to the decarbonylation reaction described in 3.2.1 above, this terminal double bond can also be formed as the result of an incomplete hydrogenation reaction. Thus, the detachment of oxygen molecules from carbon chains was not immediately followed by the bonding of hydrogen molecules. The terminal double bond formations were indicated by high iodine values in runs with catalysts 3, 4, and 5 and were also confirmed by FTIR spectra from the respective runs. The product of run with catalyst 6 turned completely into a gel at room temperature. This condition was suspected because of the rather heavy hydrocarbon content due to dimerization. Based on this phenomenon, it can be concluded that the inadequacy of potassium promoter will result in a higher chance of dimerization during the reaction, resulting in heavier than expected hydrocarbons. This might also be linked to or caused by a higher amount of coke formed that reduced the catalyst's activity, so the hydrogenation and deoxygenation reaction could not be carried out properly or completely. Therefore, the amount of potassium promoter must be sufficient enough to minimize coking on the catalyst surface, especially in the higher Ni:Mo catalyst.

Bio-hydrocarbon Products

The result of GC analysis, which indicated the yield of certain carbon chains, is shown in Table 5. Based on the GC results, the hydrocarbons produced mainly have C_{15} – C_{19} hydrocarbons as major components and, thus, were very suitable to be utilized as green diesel. The density of hydrocarbons produced is still a bit inferior if compared to Indonesia's standard for commercial biofuels or SNI-04-7182-2006 (850 – 890 kg/m^3 at 40ºC). Fortunately, the hydrocarbon's kinematic viscosity already met the standard (2.3 – 6.0 mm^2/s at 40ºC).

The final cyclopropenoid content in hydrocarbons was generally much lower (up to 99% removal) than the original kapok-seed oil. This was proved qualitatively by Besson tests that gave negative results for all products and confirmed by FTIR analysis and quantitatively by titrimetric using Dubertaki reagent, which resulting varied (0.0–0.021 mmol/g-oil) cyclopropenoid content, however, was considerably negligible if compared to the original kapok-oil (0.47 mmol/g-oil).

The saturation of kapok seed oil reduction was indicated by a significant decrease in the iodine value in all final products (between 13–41 g-I2 /100 g-oil). The remaining unsaturated content in the most products already complied with the B-30 mixture (30% FAME content, with an iodine value of a maximum of 34.5 g-I2 /100 g-oil) according to the biodiesel (FAME) standard SNI-04-7182-2006 (a maximum of 115 g-I2 /100 g-oil for B-100).

FTIR Analyses

All the FTIR spectra of the green diesel products showed that the hydrotreating process was able to bring down the cyclopropenoid content (1370-1470 cm^{-1}) significantly, as well as the carbonyl (C=O) group (1700-1750 cm^{-1}). Similar phenomena were found for C-O bonding (1160-1200 cm^{-1}) and C=C bonds (1600-1650 cm^{-1}). Figure 2 shows some of the results of the FTIR spectra of *Ceiba pentandra* seed oil as feedstock and green diesel products from run with catalyst 4 (with a relatively small conversion of 83,6%) and catalyst 7 (with a relatively high conversion of 93,2%). Only 2 samples were provided, for illustration purposes only, because the spectra of all samples were typical. The appearance and disappearance of some bands associated with chemical groups such as esters, carboxylic acids, and hydrocarbons within the products could be observed compared to raw *Ceiba pentandra* seed oil.

An interesting fact revealed from the FTIR peak around 960-980 cm^{-1} was related to the terminal alkene ($–CH=CH_2$) group in the bio-hydrocarbon chain, which was formed as a result of the removal of oxygen atoms from the carboxylic acid or ester functional groups present in the vegetable oil. The hydrogen gas reacted with the oxygen atoms in the carboxylic acid or ester functional groups, forming water and removing the oxygen from the molecule. This resulted in forming of a hydrocarbon molecule with a C=C double bond. Similarly, during the decarboxylation process, the ester group present in the vegetable oil was removed as carbon dioxide, forming a hydrocarbon with a C=C double bond. In both cases, removing the functional group involves the cleavage of the carbon-oxygen or carbon-carbon bonds within the molecule.

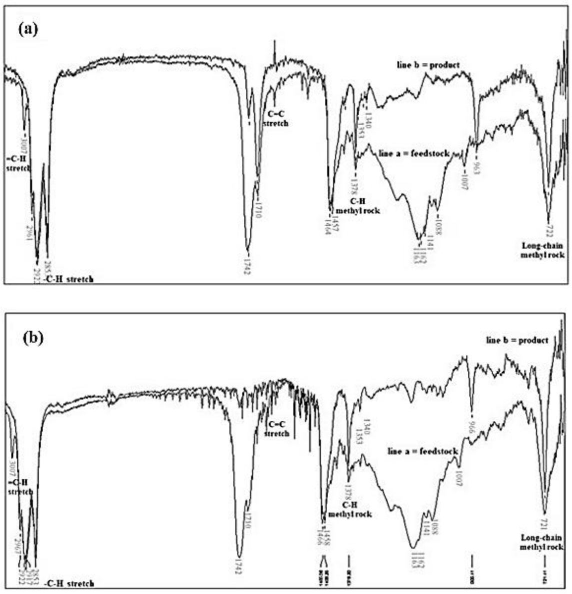

Fig. 2: FTIR spectrum of the product from catalyst: (a) 4 and (b) 7, in comparison with feedstock (line a).

The terminal alkene is relatively more reactive and possibly the cause of the dimerization at some runs. The connection between them can be judged by the products whose terminal alkene, significantly obvious from the FTIR analyses, would have darker color, greater densities, and more viscous liquid (or even with white precipitates present due to dimerization). The best green diesel product was obtained from catalyst no 8, in which the double bond was mostly saturated (reflected from the lowest Iodine value), including the terminal alkene.

Catalyst Characterization

As previously discussed, the sulfided Ni-Mo/γ-Al_2O_3 catalyst no 8 (Ni:Mo ratio 0.2 and K/P ratio 0.5) was considered as the best catalyst combination which gave the best performances such as the highest conversion (96%), lowest iodine value (13.4 g-I_2/100 g) and absence of cyclopropenoid content in hydrocarbons produced. Further characterizations were carried out to examine this particular (fresh) catalyst sample.

The BET surface area for this catalyst was 143.9 m^2/g, which is lower than pure γ-Al_2O_3, which was reported to have a surface area of 160 – 300 m^2/g (Hagen, 2006)), and 240 m^2/g (Pankaj Kumar, 2014). During the catalyst preparation process, the sulfided Ni-Mo particles might aggregate (as supported by the TEM analysis), resulting in larger particle sizes and a lower surface area.

XRD pattern of the catalyst is shown in Fig.t 3, in which diffraction peaks at 67.3 were found and associated with γ-Al_2O_3 (Fang Liu, 2007; Tiancun Xiao, 2003; Yuguang Wang, 2008). According to Lonkar *et al.* (2018), peaks at 13.34°, 33.36°, 39.86°, 49.62° and 58.69° confirm the existence of nanosized MoS_2; meanwhile, peaks at 30.71°, 35.2°, 46.2°, and 53.97° corresponding to nanosized NiS particle. The relatively strong peaks at 58.69° and especially at 46.2° were found, indicating the existence of proof of nanosized MoS_2 and NiS as active sites on synthesized catalysts.

Additionally, a relatively weak peak at 37.3° was observed in the XRD pattern indicating the existence of NiO, which is usually indicated by the presence of the peaks at 37.3°, 43.4° and 63.0° (F. J. Maldonado-Hodar, 1996; Fang Liu, 2007; Tiancun Xiao, 2003; Yuguang Wang, 2008). Wang *et al.* (2008) reported crystalline MoO_3 diffraction peaks were usually shown at 23.3°, 25.5°, 27.2° and 33.6°; in this research, a weaker peak was found at around 23° which spotted the existence of crystalline MoO_3 in our catalyst. The peak at 2θ of 14.5° was most likely associated with the well-crystallized $NiMoO_4$, which indicates that a well-crystallized metal active site was formed (Wang *et al.* 2008).

However, the Ni and Mo oxides phases were not the expected active sites for our purpose but rather showed that the sulfidation process was not 100% completed.

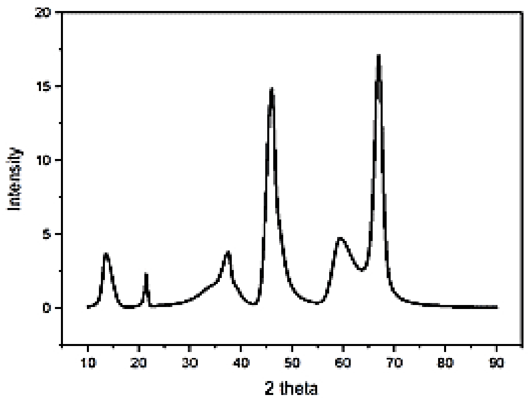

Fig. 3: XRD diffraction pattern of sulfided Ni-Mo/γ-Al_2O_3

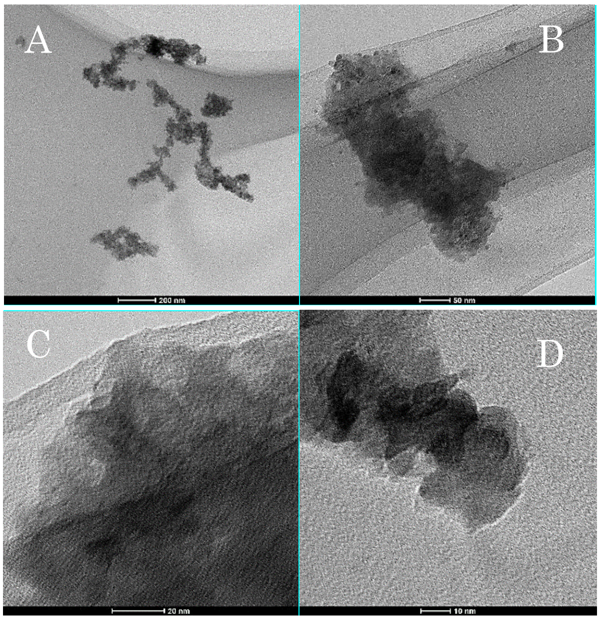

Fig. 4: TEM picture of sulfided Ni-Mo/γ-Al_2O_3

Figure 4 shows the TEM picture of the catalyst. It could be seen that the catalyst had a morphology which tended to be agglomerate (Fig 4.a). The tiny particles observed in Fig 4.b were likely nanosized NiS and MoS_2 dispersed on the support (Xiao *et al.*, 2003). However, Fig 4.b showed the catalysts exhibited a slight aggregation of the metal sulfide particles, which could result in a reduced catalytic activity and selectivity due to lower surface area and less accessible active sites. However, in the catalyst formulation P promoter had been incorporated to disperse the Mo better (as the much more dominant metal) onto the support's surface. In the TEM micrograph of the catalyst shown in Fig 4.c and 4.d, a layer of substance covering the particle catalyst was found. The layer was suspected as the result of the interaction between sulfided Ni-Mo particles and the γ-Al_2O_3 support, in which either metal-support partial penetration or even encapsulation of the sulfided Ni-Mo particles by the γ-Al_2O_3 support might occur.

CONCLUSIONS

The catalytic hydrotreating of Kapok seed oil using Sulfide Ni-Mo/γ-Al_2O_3 showed a promising result. All catalyst synthesized in this research has resulted good outcome: high conversion; good hydrocarbons saturation performance, indicated by reduction of iodine value; good hydrocarbons deoxygenation performance; and high capability to eliminate cyclopropenoid. The best Ni:Mo molar ratio was 0.2; meanwhile K:P promoter ratio was 0.5:1 which exhibited remarkable performance for hydrotreating with a high conversion of 96% and desirable product composition comprising of C_{15}-C_{19} hydrocarbons without any cyclopropenoid substance and dimerized product detected. Other catalysts with higher Ni:Mo ratios (0.33:1 and 0.4:1) required more potassium promoters than low Ni:Mo ratios to perform better. The KOH and K_2CO_3 salt gave similar potassium loading in the catalyst surface, but potassium carbonates gave superior coke prevention performance than the hydroxides. Furthermore, The FTIR and qualitative tests have confirmed that cyclopropenoid groups in the feedstock were removed completely by almost all of the catalysts. Characterization of synthesized catalyst revealed the formation of NiO, MoO_3 and $NiMoO_4$ phases and the possibility of NiS and MoS_2 particle on the catalyst. The gas chromatography of final products showed that hydrocarbons formed mainly have diesel-range hydrocarbons, but some runs gave heavier hydrocarbons (C_{20}-C_{30}) in a small amount.

ACKNOWLEDGEMENT

The authors gratefully acknowledge the funding from the Institute for Research and Community Service at Parahyangan Catholic University (LPPM UNPAR). Catalyst preparation procedures were modified from the catalyst preparation techniques developed by Prof. Dr. Ir. Subagjo in the Center of Chemical Reaction Technology and Catalysis at Bandung Institute of Technology (ITB). The authors are also thankful to Prof. Subagjo for the assistance with the GC analysis.

REFERENCES

Ameen, M., Azizan, M.T., Ramli, A., Yusup, S. & Abdullah, B., 2020. "The effect of metal loading over Ni/γ-Al_2O_3 and Mo/γ-Al_2O_3 catalysts on reaction routes of hydrodeoxygenation of rubber seed oil for green diesel production." *Catal. Today 355*, 51-64.

Anwar, F., Rashid, U., Ali Shahid, S. & Nadeem, M., 2014. "Physicochemical and Antioxidant Characteristics of Kapok (*Ceiba petandra Gaertn*.) Seed Oil." *J. Am. Oil Chem. Soc. 91 (6)*, 1047-1054.

Atanasova, P., Halachev, T., Uchytil, J. & Kraus, M., 1988. "Effect of phosphorus on the surface concentration of molybdenum and nickel in the oxide form of nickel—molybdenum/alumina catalysts and on their hydrodesulphurization activity." *Appl. Catal. 38(2)*, 235-240.

Chai, G.Y. & Falconer, J.L., 1985. "Alkali promoters on supported nickel: Effect of support, preparation, and alkali concentration." *J. Catal. 93(1)*, 152-160.

Chiappero, M., Do, P.T.M., Crossley, S., Lobban, L.L. & Resasco, D.E., 2011. "Direct conversion of triglycerides to olefins and paraffins over noble metal supported catalysts", *Fuel 90*, 1155-1165.

Choudhary, T.V. & Philips, C.B., 2011. "Renewable fuels via catalytic hydrodeoxygenation." *Appl. Catal. A: General 397*, 1-12.

Daudin, A., Bournay, L. & Chapus, T., 2013. E.U. Pat. EP 2228423B1.

Dindi, H., Sengupta, S.K., Gonzon, A.F. & Corbin, D. R., 2011. U. S. Pat. US8084655B2.

Ding, S., Jiang, S., Wang, J., Huang, X. & Yang, Z., 2020. "Effects of the Ni-Mo ratio on olefin selective hydrogenation catalyzed on Ni-Mo-S active sites: A theoretical study by DFT calculation." *Fuel 277*, 118-136.

Greenberg, A.,1982. "Cyclopropenoid Fatty Acids." *J. Chem. Educ.,* 59, pp. 539-543.

Hagen, J., 2006. Industrial Catalysis: A Practical Approach. vol. 2, 2nd ed., Wiley-VCH Verlag GmbH & Co., Weinheim. KGaA

Hudaya, T., Liana & Soerawidjaja, T.H., 2013. "A study on low temperature and pressure hydrogenation of cyclopropenoid-group containing non-edible oil for biodiesel feedstock." *Energy Procedia 32*, 209 – 215.

Iwamoto, R. & Grimblot, J., 1999. "Influence of phosphorus on the properties of alumina-based hydrotreating catalysts." *Adv. Catal. 44*, 417-503.

Kubicka, D. & Kaluza, L., 2010. "Deoxygenation of vegetable oils over sulfided Ni, Mo and NiMo catalysts.", *Appl. Catal. A 372*, 199-208.

Kumar, P., Yenumala, S.R., Maity, S.K. & Shee, D., 2014. "Kinetics of hydrodeoxygenation of stearic acid using supported nickel catalysts: Effects of supports." *Appl. Catal. A 471*, 28-38.

Liu, F., Xu, S., Cao, L., Chi, Y., Zhang, T. & Xue, D., 2007. "A comparison of NiMo/Al_2O_3 catalysts prepared by impregnation and coprecipitation methods for hydrodesulfurization of dibenzothiophene." *J. Phys. Chem. C. 111 (20)*, 7396-7402.

Lonkar, S.P., Pillai, V.V. & Alhassan, S.M., 2018. "Three-dimensional NiS-MoS_2/ Graphene heterostructured nanohybrids as high-performance hydrodesulfurization catalysts." *ACS Appl. Nano Mater. 1 (7)*, 3114–3123.

Maldonado-Hodar, F.J., Madeira, L.M.P. & Portela, M.F., 1996. "The effects of coke deposition on $NiMoO_4$ used in the oxidative dehydrogenation of butane." *J. Catal. 164 (2)*, 399-410.

Markkanen, V., Lindqvist, P., Harlin, E., Aalto, P., Myllyoja, J. & Alopaeus, V., 2009. Canada Pat. CA2729651C.

Mohammad, M., Hari, T.K., Yaakob, Z, Sharma, Y.C. & Sopian, K., 2013. "Overview on the production of paraffin based-biofuels via catalytic hydrodeoxygenation." *Renew. Sustain. Energy Rev. 22*, 121-132.

Santillan-Jimenez, E. & Crocker, M., 2012. "Catalytic deoxygenation of fatty acids and their derivatives to hydrocarbon fuels via decarboxylation/decarbonylation." *J. Chem. Technol. Biotechnol. 87(8)*, 1041-1050.

Senol, O.I., Viljava, T.R & Krause, A.O.I., 2007. "Effect of Sulphiding Agents on the Hydrodeoxygenation of Aliphatic Esters on Sulphided Catalysts." *Appl. Catal. A 326 (2)*, 236-244.

Toba, M., Abe, Y., Kuramochi, H., Osako, M., Mochizuki, T. & Yoshimura, Y., 2011. "Hydrodeoxygenation of waste vegetable oil over sulfide catalysts." *Catal. Today 164*, 533-537.

Vonortas, A., Kubicka., D. & Papayannakos, N., 2014. "Catalytic co-hydroprocessing of gasoil–palm oil/AVO mixtures over a NiMo/γ-Al_2O_3 catalyst." *Fuel 116*, 49-55, 2014.

Wang, H., 2012. Biofuels production from hydrotreating of vegetable oil using supported noble metals, and transition metal carbide and nitride. Doctor of Philosophy Thesis, Wayne State University.

Wang, Y., Xiong, G., Liu, X., Yu, X., Liu, L., Wang, J., Feng, Z. & Li, C., 2008. "Structure and reducibility of NiO-MoO_3/γ-Al_2O_3 catalysts: Effects of Loading and Molar Ratio." *J. Phys. Chem. C 112*, 17265-17271.

Wua, W., Fan, Q., Yi, B., Liua, B. & Jianga, R., 2020. "Catalytic characteristics of a Ni–MgO/HZSM-5 catalyst for steam reforming of toluene." *RSC Adv. 10*, 20872-20881, 2020.

Xiao, T., Suhartanto, T., York, A.P.E., Sloan, J. & Green, M.L.H., 2003. "Effect of molybdenum additives on the performance of supported nickel catalysts for methane dry reforming.", *Appl. Catal. A 253(1),* 225-235, 2003